Dust Eruptions by Photophoresis and Solid State Greenhouse Effects

Gerhard Wurm* and Oliver Krauss

Institute for Planetology, University of Münster, Wilhelm-Klemm-Strasse 10, 48149 Münster, Germany

(Received 9 September 2005; published 6 April 2006)

We carried out experiments that show a gas pressure dependent ability of light to eject particles from a dust bed. Dust eruptions also occur upon removal of the light source. This can be attributed to a solid state greenhouse effect and photophoretic forces. This ejection mechanism works at light intensities larger than 6 kW/m^2 but in extreme cases might work as low as 1 kW/m^2. It can be applied to sunlit dust on Mars where it aids or triggers dust lift-off from the surface into the atmosphere. It is of importance for dusty bodies at the inner edge of protoplanetary disks where it leads to light induced erosion. The effect also offers a base for technical applications of dust removal in low pressure environments.

DOI: 10.1103/PhysRevLett.96.134301 PACS numbers: 44.30.+v, 47.45.Gx, 95.30.Wi, 96.12.Jt

It has long been known that temperature gradients across a free particle can lead to its efficient motion in a low pressure gaseous environment [1–5]. The effect is caused by a difference in momentum transfer from the gas molecules at different surface temperatures, called thermophoresis. If the mean free path of the gas molecules is smaller than the particle (continuum flow regime) the thermophoretic force is given as [2]

$$F_{\mathrm{Ph}} = -\frac{3\pi\eta^2 d}{2T\rho_g}\frac{dT}{dx}. \quad (1)$$

Here, η is the gas dynamical viscosity, d is the particle size, T is the gas temperature, ρ_g is the gas density, and dT/dx is the temperature gradient across the particle. In the free molecular flow regime the force *increases* linearly with pressure p [4,6].

Temperature gradients also develop in the surface layers of a larger body upon illumination. It has to be noted that a partly transparent body does not necessarily get hottest at the surface but might heat up some distance below. This effect has been termed the solid state greenhouse effect [7–12]. In a porous dust bed light is transferred to deeper particle layers through the pores of the dust bed by forward light scattering, and a solid state greenhouse effect can be established for the topmost dust layers as discussed below.

Experiments. In view of such temperature gradients dust particles are subject to a thermophoretic force away from the surface. With respect to the light as heat source we will further call the effect photophoresis. If the photophoretic force is stronger than gravity and cohesion particles should be lifted. To test this hypothesis, we place different powders on a horizontal surface in a chamber which we slowly evacuate. We illuminate the several mm deep dust bed with a focused laser beam (maximum 120 kW/m^2). Intense fountains of material are ejected from the surface at low pressure at the illuminated spot (Fig. 1). Eruptions vary in time from instantaneous upon irradiation to being delayed by up to a few seconds (visual observation). In general, the ejection at a given spot stops after carving a crater of up to several mm depth.

The effect is strongly pressure dependent. To quantify this we illuminate randomly chosen spots on the surface of a graphite dust bed. We observe the surface under a microscope while we turn on the laser beam. At a certain pressure significant (inelastic) motion or eruption can be observed on every spot chosen. With dust samples always prepared the same way these threshold pressures correspond to the same average photophoretic forces. We have repeated the procedure for different radiation fluxes I. Starting with full laser power I_0, we successively placed gray filters in front of the laser. If the photophoretic forces are proportional to the radiation flux we thus get a pressure dependence of the photophoretic force at the full intensity as I_0/I (Fig. 2). Particle motion could clearly be detected at intensities as low as 6 kW/m^2 and below but the experiments are not suited to determine the lowest radiation flux, at which particle lift-off is possible. Experiments on levi-

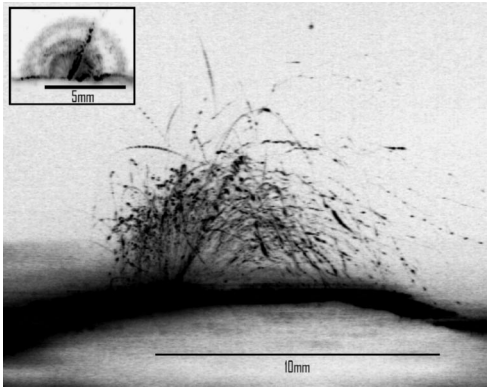

FIG. 1. Fountains of particles erupting due to illumination with a red laser beam. The large image is for a commercial graphite powder. The pressure in the chamber is 10 mbar. The laser is heading from upper right to lower left. Particles are visualized by a laser curtain in the focal plane. The images are long exposures, while the target dust was slowly moved to initiate a number of eruptions. The asymmetry is due to motion of the experiment chamber. The inset is for a powder of spherical vitreous carbon at about 150 mbar gas pressure. Three eruptions can be distinguished as different shells in the image.

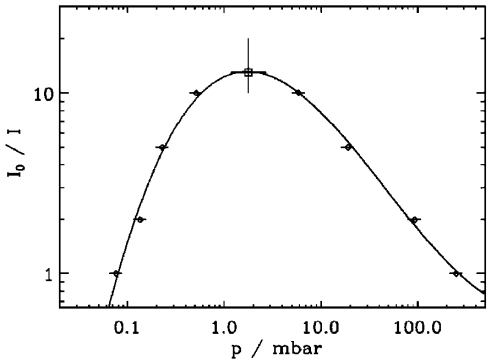

FIG. 2. Measured pressure dependence of the threshold intensities for particle motion at the surface of a graphite dust bed. The line is a polynomial fit of 3rd order to guide the eye. The light intensities have no significant error since we used calibrated gray filters and always the same laser. The highest radiation flux was $I_0 = 120\ \mathrm{kW/m^2}$. For the lowest laser intensity (highest I_0/I value) an error bar in relative intensity has been assigned since a 100% threshold for dust motion or eruption was not achieved.

tated graphite aggregates suggest that laser intensities as low as $1\ \mathrm{kW/m^2}$ result in lift forces larger than gravity. However, since these are unpublished results the value is only speculative so far.

We qualitatively tested other dust samples (Table I). Every ''dark'' powder erupted. Only nonabsorbing white SiO_2 particles did not get ejected. New explosions at a given (cratered) spot also occurred when the laser was turned off. They can eject a larger amount of material than the initial photophoretic eruption at the same spot.

Model. The effect of dust eruptions by light at low pressure can qualitatively be explained in terms of a solid state greenhouse effect and photophoretic forces. To support this explanation we model the heat transfer in the dust bed in accordance with our experimental settings. Upon illumination the temperature T of the dust bed changes in time t as

$$\frac{\partial T}{\partial t} = \frac{k_b}{\rho_b c_b}\nabla^2 T + Q. \tag{2}$$

Here, k_b is the thermal conductivity, ρ_b is the mass density, and c_b is the heat capacity of the dust bed. Q is the heat source, i.e., the absorbed laser light. We assume a homogeneous beam profile with a circular cross section and an exponential decay of the radiation within the dust bed. The absorbed power per volume as heat source Q is given as

$$Q = \frac{I}{l} e^{-x/l} \tag{3}$$

with l being the absorption length and x the coordinate perpendicular to the surface. In a granular medium radiation travels unchanged through the pores. In addition, a significant part of the light interacting with the dust is scattered mostly in a forward direction due to the large size of the particles compared to the wavelength. Therefore, light can penetrate into the dust bed. The absorption length l depends on the morphology (porosity, clumpiness) of the dust bed. Typical porosities of dust beds in our earlier works are 0.8 [13]. This applies to the graphite discussed above. We did not determine the porosities otherwise since even manually compressed dust beds have high porosities larger than 0.65 [14]. Therefore, the absorption length is always a few times the size of the particle clumps making up the target [7]. However, without loss of generality we consider $l = 1$ mm. This accounts for some degree of clumping of micron-sized dust. The models show that a few times larger absorption length does not change the principle result.

We solved Eq. (2) for a model dust cube of 1 cm length. In the center we included a 1 mm cylindrical heat source according to Eq. (3). At 5 mm depth the absorbed radiation is well below 1% of the surface radiation and we do not consider heating at larger depths to be important. Therefore, we cut the heat source off at 5 mm depth. We assumed $I = 63\ \mathrm{kW\,m^{-2}}$ (50 mW laser power). The box has insulating sides and bottom and initially $T = 293$ K. The thermal conductivity combines the thermal conductivities of particles, gas, and radiation transport within the pores. For highly porous graphite powder the particle's conductivity can be as low as $k_p = 0.016\ \mathrm{W\,m^{-1}\,K^{-1}}$ [5]. The thermal conductivity of the gas depends on the gas pressure but a typical value in the pressure range used, combining low particle conductivity and gas conductivity, would be $k_b = 0.05\ \mathrm{W\,m^{-1}\,K^{-1}}$ [15]. Radiation transport through pores can be modeled by an effective thermal conductivity which is [16]

$$k_R = 4\sigma\varepsilon n^2 T^3 R. \tag{4}$$

Here, σ is the Stefan-Boltzmann constant, ε is the emissivity of the walls, n is the refractive index of the gas, and R is the pore size. Assuming 100 μm pores, emissivity and refractive index to be approximately 1, and a maximum temperature of 450 K, it is $k_R = 0.002\ \mathrm{W\,m^{-1}\,K^{-1}}$. This is low compared to the other conductivities and we neglect conduction by thermal radiation transport [2,17]. The density of the dust bed is $\rho_b = 0.45\ \mathrm{g\,cm^{-3}}$ and the heat capacity is $c_b = 712\ \mathrm{W\,Kg^{-1}\,K^{-1}}$. As a boundary condition for the surface we assume heat flux according to thermal emission and absorption of thermal radiation of the surroundings at $T = 293$ K. The $3d$ transient heat transfer is calculated using a commercial software package

TABLE I. Basic parameters of used dust samples.

Material	Particle Size (μm)	Color
Graphite	0.1–10 (platelike)	black
Graphite	<100 (platelike)	black
Vitreous Carbon	0.1–12 (spherical)	black
Corundum	16.3–18.3	gray
Iron Oxides	<100	red, black, brown
Basalt	<100	gray
SiO_2	1.5 (spherical)	white
SiO_2	<10 (1–5, 80%)	white

[18]. Figure 3 pictures the temperature profile on the cylinder (heat source) axis at 3 different times.

Essentially the temperature profile decreases with depth as might be expected. However, in agreement to other models of nonsurface light absorption (e.g., Ref. [8]) we get a reversed temperature gradient in the topmost part of the dust bed. Even if this layer is only about 100 μm thick after 10 s this is up to several tens of particle layers. The temperature gradient at the center of the surface reaches $dT/dx = -1.5 \times 10^4$ Km^{-1} at $t = 1$ s. At $t = 10$ s the surface gradient is $dT/dx = -4 \times 10^4$ Km^{-1} but decreases only slowly further on.

The permeability of gas for a thin porous dust layer is fairly high. Therefore, locally the gas moves freely around the individual dust particles in the uppermost layers of a dust bed. The temperature gradient thus induces a photophoretic force according to Eq. (1) for the individual dust particles. Using $dT/dx = -1 \times 10^4$ Km^{-1}, $\eta = 1.8 \times 10^{-5}$ kg^{-1} ms^{-1}, $d = 1$ μm, $\rho_g = 0.12$ kg m^{-3} ($p =$ 100 mbar), and $T = 380$ K yields $F_{\mathrm{Ph}} = 3.3 \times 10^{-13}$ N. With $\rho_p = 2.25$ g cm^{-3} the gravitational force acting on this particle is $F_g = 9.2 \times 10^{-14}$ N. Photophoretic forces are thus dominating over gravitational forces shortly after illumination starts. Ejection of particles occurs as soon as the total lift on a particle sample is overcoming the cohesive forces at their weakest points. The pull-off force for a micron-size (spherical) particle is on the order of 10^{-7} N [19]. Thus typically 10^6 particles are needed to overcome cohesion. This is just a rough estimate since aggregates are probably bound by more than one contact, but then the weight of flake like particles is lower and the pull-off forces also vary statistically. Not individual grains but aggregates of tens or hundreds of micrometers in size are eventually ejected. We note that this assumes that photophoresis acts on each constituent grain according to its properties, i.e., its size, not the size of the aggregate. Thus a 100 μm aggregate has a total lift force of 10^6 times the lift force of an 1 μm grain not just 100 times as a compact 100 μm grain would have according to Eq. (1).

However, as the photophoretic and the gravitational force are comparable in the model, at slightly higher gas pressure gravity will dominate. This is in good agreement with our measurements that ejection of graphite particles at maximum radiation flux starts at about 100 mbar.

Once cohesion is overcome particles and aggregates are accelerated (erupt) rather than being released smoothly. The temperature gradient significantly changes up to several seconds after illumination starts. In agreement with the experiments, if the photophoretic and the gravitational force are comparable the particles might only reach the threshold and be ejected up to seconds after the laser is turned on.

Photophoresis works best at a gas pressure where the mean free path of the gas molecules is about the size of the particles. For particles of several micrometers in size the maximum force would occur at several mbar, which is also in good agreement with the measurements (Fig. 2). As expected from theory the photophoretic force increases linearly with pressure at low pressures (Fig. 2). At larger pressure the decrease is more flat than expected from Eq. (1). However, the graphite powder has a wide size distribution with particles down to below 100 nm. Thus, Fig. 2 results from a superposition of different forces with maxima at different positions. Also, the thermal conductivity changes with gas pressure at larger values [15]. To disentangle this is beyond the scope of this Letter.

Figure 4 shows the evolution of the temperature gradient at the center of the illuminated spot after the heat source (laser) is turned off. While the maximum temperature gradient at the surface decreases (absolute), the depth at which the temperature gradient changes its sign moves quickly deeper into the dust bed. Therefore, the photophoretic pull integrated over several particle layers will even get stronger further below the surface (below 80 μm after 0.1 s) if the laser is turned off. Larger aggregates can be ejected in agreement with the experiments.

It has to be noted that a *radial* temperature gradient also develops due to the localized nature of the light source. Model values at the edge of the illuminated surface range up to 10 times the lifting temperature gradient and surface eruptions are not strongly correlated to the surface normal

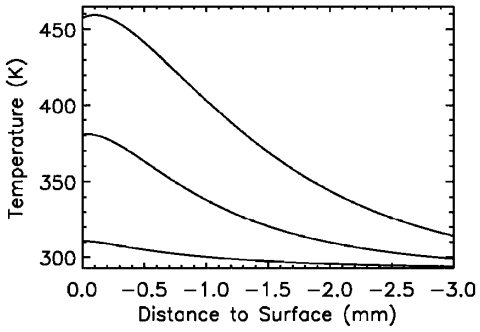

FIG. 3. Model temperature profiles on a vertical line through the center of the dust bed at $t = 0.1$ s, 1 s, and 10 s after the laser is turned on (from bottom to top).

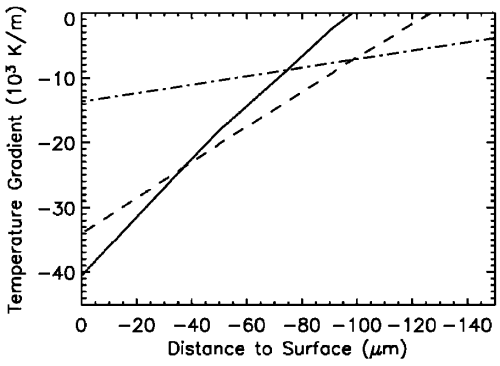

FIG. 4. Model temperature gradients on a vertical line through the center of the dust box. Solid line: after 10 s of illumination, laser is turned off. Dashed line: 0.1 s after the laser is turned off. Dash-dotted line: 1 s after laser is turned off.

nor to the direction of the radiation (e.g., inset in Fig. 1). Particles within a crater cannot move as easily since this sideward component and the passive particle layers on top would eventually allow no more motion. In addition, simulations of a dust bed including a cylindrical hole as crater model (1 mm wide, 2.5 mm deep) show that heat at the edges is also efficiently transferred to the adjacent regions (crater walls). The temperature gradient after $t = 1$ s is about 1 order of magnitude smaller at the crater bottom. Pointlike illumination is not a prerequisite for photophoretic lift. If the whole surface is illuminated similar vertical temperature profiles result in $3d$ as well as in the analog $1d$ model.

We exclude other effects as explanation for the eruptions. The effect is visible for dry samples after being heated several hours at 120° C. Thus, water vapor, e.g., produced during heating plays no role. Expansion of the gas heated by the dust is also not important. The high permeability of the porous dust bed leads to a rapid adjustment of the gas pressure in contrast to ejections still occurring after seconds. Also, no water vapor or gas expansion effect should be initiated after the laser is turned off. The characteristic pressure dependence (Fig. 2) rules out further expansion of the gas. It also rules out expansion of the dust bed, radiation pressure, and charge effects from being responsible, since they should all work at vacuum. In addition photoelectric charging is only possible at uv wavelengths. We thus conclude that the illumination of a dusty surface at reduced pressure can lead to a small scale solid state greenhouse effect and subsequent photophoretic eruptions of dust.

Applications. Photophoretic ejection has a number of applications. In the current models of planet formation dust in protoplanetary gas-dust disks is growing to larger dust aggregates through mutual collisions [20,21]. In the late stage of protoplanetary disk evolution photophoresis might lead to the formation of dust rings that are observed around young stars, and probably trigger the formation of the Kuiper belt or asteroids [22,23]. It is likely that the surfaces of the first dusty bodies are susceptible to photophoretic eruptions. At the luminous conditions and at pressures of sub-mbar in the inner regions of the disk [24] the mechanism most probably results in the ejection of dust and, thus, erosion. The surface gas pressure on Mars is about 10 mbar [25]. The average radiation flux by sunlight is about $I = 600\ \mathrm{W/m^2}$. This is about a factor of 10 below the observed threshold for particle ejection in our experiments. However, the lower threshold could not be detected well and as speculated above it might be as low as $1\ \mathrm{kW/m^2}$. It should be considered that the gravitational acceleration on Mars is only about $1/3$ of Earth's gravity. Even if the flux is slightly too low to eject particles, photophoretic lift will aid motion of dust particles by wind, especially as Mars is close to its perihelion when the flux is increased to above $I = 700\ \mathrm{W/m^2}$ [26]. A further application might be removal of dust from optical surfaces or solar panels on Mars exploration missions. If, e.g., lenses are used the necessary intensities can easily be reached to eject particles. As seen, within a dust surface a large body shows photophoretic features of its constituents. One might think of creating an artificial surface with much stronger, optimized photophoretic forces. In analogy to solar sails based on radiation pressure solar sails based on photophoresis could be much stronger. These could, e.g., be used for propulsion of small probes on Mars or in Earth's stratosphere. For particle removal the effect might also have other technical and industrial applications.

This work is funded by the Deutsche Forschungsgemeinschaft.

*To whom all correspondence should be addressed.
E-mail address: gwurm@uni-muenster.de

[1] W. Crookes, Proc. Phys. Soc. London **1**, 35 (1874).
[2] I. I. Kantorovich and E. Bar-Ziv, Fuel **78**, 279 (1999).
[3] F. Ehrenhaft, Ann. Phys. (Leipzig) **56**, 81 (1918).
[4] S. Beresnev, V. Chernyak, and G. Fomyagin, Phys. Fluids A **5**, 2043 (1993).
[5] H. Rohatschek, J. Aerosol Sci. **16**, 29 (1985).
[6] N. T. Tong, J. Colloid Interface Sci. **51**, 143 (1975).
[7] B. J. R. Davidsson and Y. V. Skorov, Icarus **156**, 223 (2002).
[8] B. J. R. Davidsson and Y. V. Skorov, Icarus **159**, 239 (2002).
[9] E. Niederdörfer, Meteorol. Z. **50**, 201 (1933).
[10] E. Kaufmann, N. I. Kömle, and G. Kargl, Adv. Space Res. (to be published).
[11] E. Kaufmann, N. I. Kömle, and G. Kargl, ESA SP **518**, 87 (2002).
[12] D. L. Matson and R. H. Brown, Icarus **77**, 67 (1989).
[13] G. Wurm, G. Paraskov, and O. Krauss, Phys. Rev. E **71**, 021304 (2005).
[14] J. Blum and R. Schräpler, Phys. Rev. Lett. **93**, 115503 (2004).
[15] M. A. Presley and P. R. Christensen, J. Geophys. Res. **102**, 6535 (1997).
[16] T. H. Bauer, Int. J. Heat Mass Transfer **36**, 4181 (1993).
[17] X. Zhang, A. Dukhan, I. I. Kantorovich, and E. Bar-Ziv, Combust. Flame **113**, 519 (1998).
[18] Femlab 3.0a Release Notes, Copyright 1994-2004 by COMSOL AB.
[19] L.-O. Heim, J. Blum, M. Preuss, and H.-J. Butt, Phys. Rev. Lett. **83**, 3328 (1999).
[20] S. J. Weidenschilling and J. N. Cuzzi, in *Protostars and Planets III*, edited by E. Levy and J. I. Lunine (University of Arizona Press, Tucson, 1993), p. 1031.
[21] G. Wurm, ESA SP **539**, 151 (2003).
[22] O. Krauss and G. Wurm, Astrophys. J. **630**, 1088 (2005).
[23] G. Wurm and O. Krauss, Icarus **180**, 487 (2006).
[24] J. A. Wood, Space Sci. Rev. **92**, 87 (2000).
[25] R. W. Zurek, in *Mars*, edited by H. H. Kieffer, B. M. Jakosky, C. W. Snyder, and M. S. Matthews (University of Arizona Press, Tucson, 1992), p. 799.
[26] R. A. Kahn, T. Z. Martin, and R. W. Zurek, in *Mars*, edited by H. H. Kieffer, B. M. Jakosky, C. W. Snyder, and M. S. Matthews (University of Arizona Press, Tucson, 1992), p. 1017.